

# CORRELATION BETWEEN HEAT TRANSFER AND FLUCTUATING PRESSURE IN SEPARATED REGION OF A CIRCULAR CYLINDER

T. IGARASHI

Department of Mechanical Engineering, The National Defense Academy, Yokosuka 239, Japan

(Received 19 July 1983 and in revised form 22 August 1983)

**Abstract**—The wake of a circular cylinder was controlled in two ways: by setting up two small cylinders inside the separated shear layers and by placing a splitter plate behind the cylinder. The former controlled the shake of the shear layers, the latter controlled the vortex formation region. The relationship between the heat transfer in the separated regions and the flow characteristics in connection with the fluctuating components of the flow, was investigated. It was found that the R.M.S. fluctuating pressure at the rear stagnation point was one of the most dominant factors of the heat transfer in the separated regions.

## NOMENCLATURE

$a, b$	length and thickness of splitter plate
$C_p$	pressure coefficient, $(p - p_0)/0.5\rho u_0^2$
$C_{pb}$	base pressure coefficient, $(p_b - p_0)/0.5\rho u_0^2$
$d$	diameter of circular cylinder
$d_0$	diameter of small circular cylinder
$d_w$	wake width (distance between free stream lines)
$g$	gap between cylinder and plate
$h, \bar{h}$	local and average heat transfer coefficients
$K$	base pressure parameter, $(1 - C_{pb})^{0.5}$
$L_v$	longitudinal length of vortex formation region
$Nu, \bar{Nu}$	local and average Nusselt number, $hd/\lambda, \bar{h}\bar{d}/\lambda$
$p, p_0$	static pressure and free stream static pressure
$p'$	fluctuating pressure
$\Delta p$	R.M.S. of fluctuating pressure, $(\overline{p'^2})^{0.5}$
$Re$	Reynolds number, $u_0 d/\nu$
$Re^*$	modified Reynolds number, $u_s d/\nu = K Re$
$S$	Strouhal number
$u_0$	free stream velocity
$u_s$	velocity along free stream line at separation point, $Ku_0$ .

## Greek symbols

$\lambda$	thermal conductivity of fluid
$\nu$	kinematic viscosity of fluid
$\rho$	density of fluid
$\phi$	circumferential angle on cylinder.

## Subscripts

b	base
r	rear stagnation point
s	separation point.

## 1. INTRODUCTION

MANY experimental investigations on the fluid flow and heat transfer in the separated region of bluff bodies have been undertaken [1-7]. The heat transfer can be expressed by the Reynolds number, the base pressure parameter and the wake width [1-4]. On the other hand, it has been reported that the heat transfer in the separated region of a circular cylinder with a wake splitter plate is reduced by about 30-35% [5, 6]. The preceding flow characteristics do not allow an estimate of the reduction to be made. From the viewpoint aforementioned or to clarify the heat transfer mechanism in the separated region, the author [8-10] has carried out a series of studies with the object of finding a new factor which dominates the heat transfer associated with the unsteadiness of the fluid flow. In ref. [8], it was suggested that the values of the R.M.S. fluctuating pressure was such a new factor. The R.M.S. values in ref. [9] explained qualitatively the characteristics of the heat transfer of a circular cylinder with a wake splitter plate. Mabuchi *et al.* [6] concluded that the vortex shedding frequency has no influence with respect to the heat or mass transfer at the rear stagnation point, however, the process of deriving their conclusion is questioned in ref. [9]. On the other hand [11], the flow pattern around a circular cylinder with a wake splitter plate differs remarkably from that in the absence of the plate. A wake control of a circular cylinder was performed by setting up two small cylinders inside the separated shear layers of the cylinder for a case maintaining the flow field of a circular cylinder [10]. In this manner, an obvious quantitative relation between the heat transfer coefficient and the values of the R.M.S. fluctuating pressure can be derived.

This paper is concerned with the previous reports [8-10] and results of subsequent research. The wake of

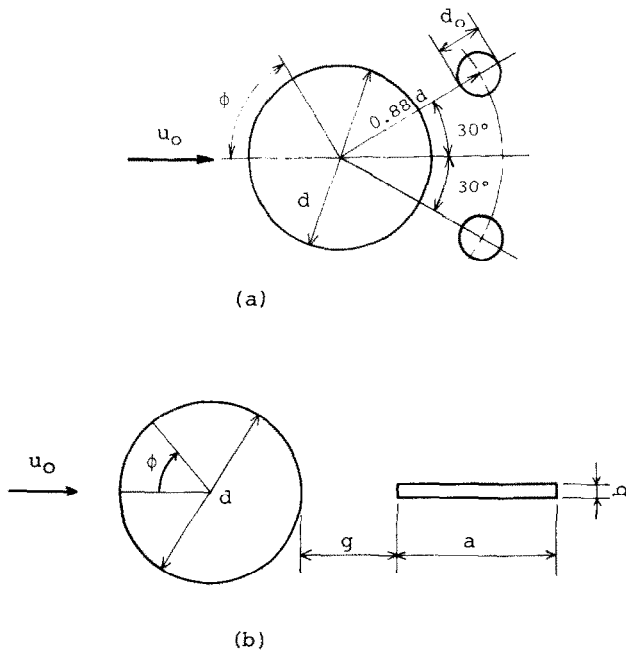


FIG. 1. Arrangement of the models and symbols.

a circular cylinder was controlled in two ways. One way used a set-up of two small cylinders inside the separated shear layers and the other placed a splitter plate behind the cylinder: the former for controlling the shake of the shear layers, the latter for controlling the position of the vortex formation region.

2. EXPERIMENTAL APPARATUS AND PROCEDURE

The experiments were performed in a wind tunnel with a working section 400 mm high and 150 mm wide. The free stream velocity,  $u_0$ , ranged from 6 to 20 m s<sup>-1</sup>, and the turbulence intensity was 0.5% in this range. The diameter of the cylinder used for flow characteristic measurements was 34 mm and that for heat transfer characteristics 34.6 mm. Therefore, the Reynolds numbers were in the range  $1.3 \times 10^4 \leq Re \leq 4.4 \times 10^4$ . Two small cylinders were at first set up inside the separated shear layers from the larger cylinder, as shown in Fig. 1(a). The diameters of the small cylinder were  $d_0 = 4, 5, 6, 8$ , and 10 mm, and the ratios of  $d_0/d$  were varied from 0.118 to 0.294. Next, as shown in Fig. 1(b), a splitter plate was placed downstream of the cylinder, and the gap between the cylinder and the plate was varied. The plates,  $b = 3$  mm thick, were of five different lengths,  $a = 10, 15, 20, 30$ , and 50 mm ( $a/d = 0.29, 0.44, 0.59, 0.88$ , and 1.47, respectively). Measurements of the heat transfer were performed under constant heat flux. Both the distribution of the time-averaged pressure and the R.M.S. fluctuating pressure around the cylinder were measured by a manometer and by a semi-conductor pressure converter connected with a pressure tap, 0.6 mm in diameter, respectively. The velocity fluctuations of the

separated shear layers were measured using a hot-wire anemometer. The wake width defined as the distance between free stream lines was obtained from the distribution of the R.M.S. velocity fluctuations. In addition, the Strouhal numbers of the vortex shedding from the cylinder were obtained from the frequency analysis of the velocity fluctuations.

3. CONTROL OF SEPARATED SHEAR LAYERS

3.1. Heat transfer

The effect of small cylinders on the local heat transfer around the cylinder is shown in Fig. 2. It is seen that small cylinders have no effect on the front surface. On the contrary, the heat transfer at the rear side is affected

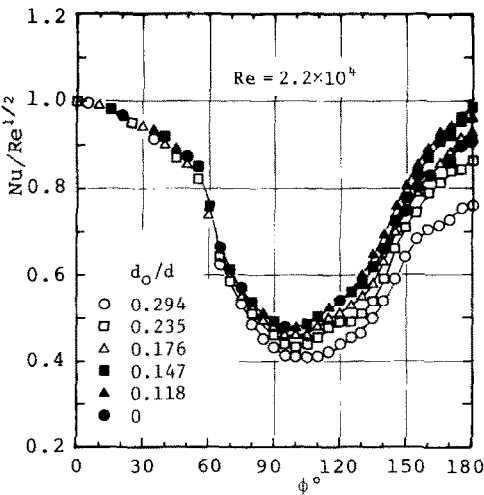


FIG. 2. Variation of local Nusselt number around a circular cylinder with small cylinders.

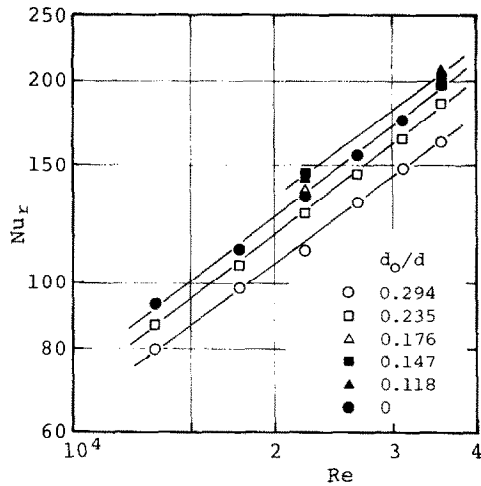


FIG. 3. Local Nusselt number at the rear stagnation point.

remarkably. In this study discussions are confined to the heat transfer in the separated region. For  $d_o/d = 0.118$  and  $0.147$ , the local heat transfer is slightly higher than that obtained in the absence of small cylinders. For  $d_o/d = 0.235$  and  $0.294$ , the local heat transfer is considerably lower than that of the single cylinder. Figure 3 shows the local heat transfer at the rear stagnation point. It satisfies the basic relation  $Nu \propto Re^{2/3}$  in agreement with the former results of bluff bodies [1-4].

3.2. Flow characteristics and heat transfer

The effects of small cylinders on the Strouhal number, base pressure parameter and wake width of the cylinder are shown in Fig. 4. The local values of  $Nu$  at the rear stagnation point of a circular cylinder in an air stream is given by [4]

$$Nu = 0.10 [2/(d_w/d)]^{1/3} (K Re)^{2/3},$$
$$Nu = 0.10 [2/(d_w/d)]^{1/3} Re^{*2/3}, \tag{1}$$

or

$$Nu = 0.12 [Re^*(d_w/d)^{-1/2}]^{2/3}. \tag{2}$$

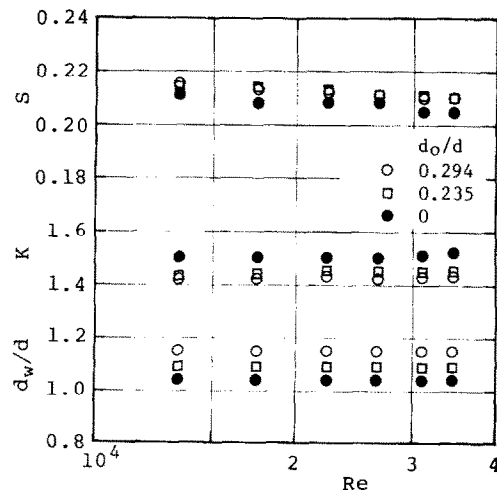


FIG. 4. Flow characteristics.

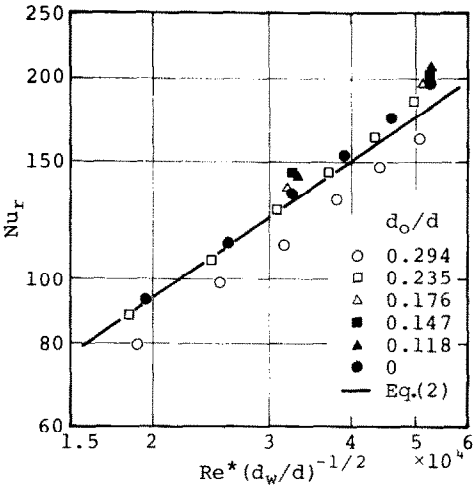


FIG. 5. Local Nusselt number at the rear stagnation point in consideration of flow characteristics.

By considering the change of the flow characteristics, shown in Fig. 4, a comparison of the experimental values with the values calculated from equation (2) is given in Fig. 5. The experimental values for  $d_o/d \leq 0.235$  agree well with the values predicted from equation (2), while those of  $d_o/d = 0.294$  are about 10% lower than the estimated values. As is obvious from the figure, for small wake control effects one can predict the reduction of the heat transfer by equation (2), but in the case of a large effect equation (2) is not sufficient to estimate the reduction quantitatively. Thus, it is necessary to introduce a new factor associated with the unsteadiness, that is, the fluctuating component of the flow. In refs. [9, 10], it becomes clear that the R.M.S. fluctuating pressure is one of the factors.

3.3. A new factor dominating heat transfer—R.M.S. fluctuating pressure

Figure 6 shows typical distributions of the R.M.S. fluctuating pressure. The profile has a peak,  $\Delta p_r$ , near the separation point. The value on the rear surface of

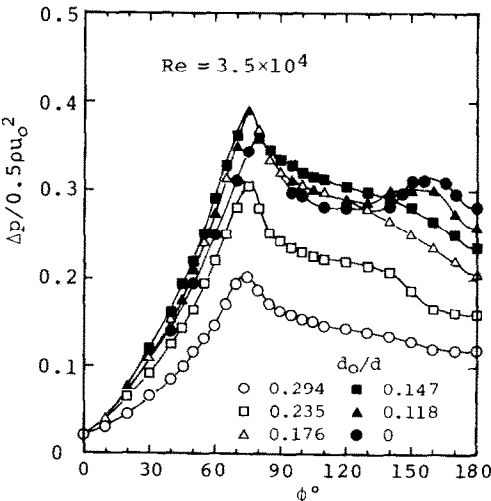


FIG. 6. Distributions of R.M.S. fluctuating pressure.

the cylinder is considerably larger than that on the front surface. Although the R.M.S. value at the rear stagnation point,  $\Delta p_r$ , of a single cylinder is about  $0.80 \Delta p_s$ , the value decreases to  $(0.55\text{--}0.65) \Delta p_s$  by setting up the small cylinders. The effects of the free stream velocity,  $u_0$ , on the R.M.S. values of  $\Delta p_s$  and  $\Delta p_r$  are shown in Figs. 7(a) and (b), respectively. The dependencies of  $\Delta p_s$  and  $\Delta p_r$  on  $u_0$  can be expressed as

$$\begin{aligned} \Delta p_s &= f(d_0/d) \cdot u_0^{2.2}, \\ \Delta p_r &= f(d_0/d) \cdot u_0^{2.2}, \quad \Delta p_r = f(0) \cdot u_0^{2.5}. \end{aligned} \tag{3}$$

These values are evidently affected by the presence of the two small cylinders. While the time-averaged pressure ( $p - p_0$ ) is proportional to the dynamic pressure,  $0.5\rho u_0^2$ , the R.M.S. fluctuating pressure,  $\Delta p$ , is not so. The maximum value of  $\Delta p_s$  is given as

$$\Delta p_s / 0.5\rho u_0^2 = C Re^{0.2}.$$

Comparing Fig. 7 with Fig. 3, the Nusselt number varies as the R.M.S. fluctuating pressure. The correlations of  $\Delta p_r$  and  $\Delta p_s$  with the local and average heat transfer coefficients on the rear surface,  $h_r$  and  $h_b$ , are shown in Figs. 8(a) and (b), respectively. Comparing the value of  $\Delta p_r$  in the presence of the small cylinders with that in their absence, there exists a difference in value between the two R.M.S. fluctuating pressures. From the plot for the maximum values of  $\Delta p_s$ , the heat transfer coefficient on the rear surface of the cylinder

can be given by the maximum R.M.S. fluctuating pressure, regardless of the presence of the small cylinders. As the unsteadiness of the flow in the separated region takes either an increase in power or a decrease by controlling the separated shear layers, the maximum R.M.S. fluctuating pressure increases or decreases. This corresponds to an increase or a decrease in the free stream velocity,  $u_0$ , and accordingly the heat transfer coefficient varies in proportion to  $u_0$ .

The local heat transfer coefficient at the rear stagnation point is related to the maximum value of  $\Delta p_s$  as follows

$$h_r \propto \Delta p_s^{0.31}, \tag{5}$$

and the average and local heat transfer coefficients are correlated by

$$\overline{h_b} = 0.7h_r. \tag{6}$$

It can be concluded that the maximum R.M.S. fluctuating pressure near the separation point,  $\Delta p_s$ , is an important factor in place of the velocity along the free stream line at the separation point,  $u_s$ , for the heat transfer in the separated region.

4. CONTROL OF VORTEX FORMATION REGION

4.1. Flow characteristics

Since the characteristics of the flow around a circular cylinder with a wake splitter plate have been described

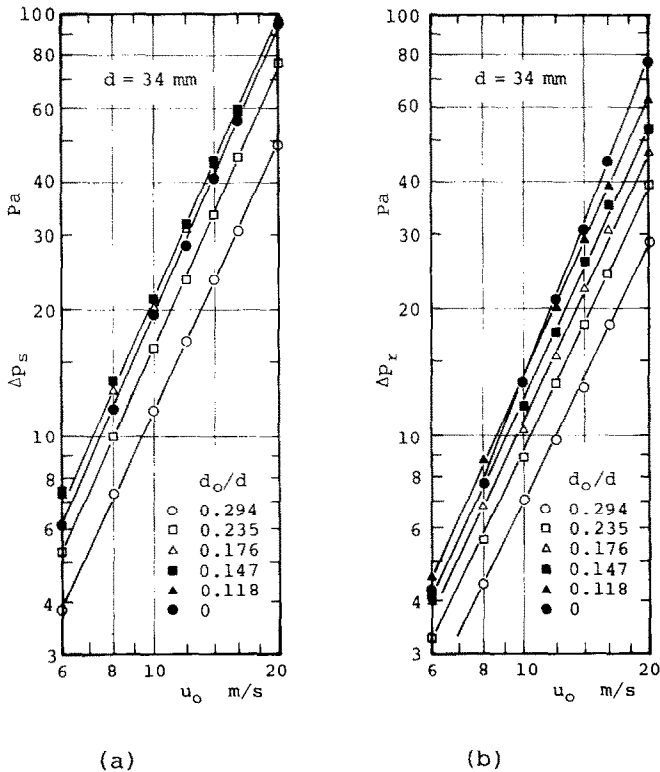


FIG. 7. Correlations of  $\Delta p_s$  and  $\Delta p_r$  vs  $u_0$ .

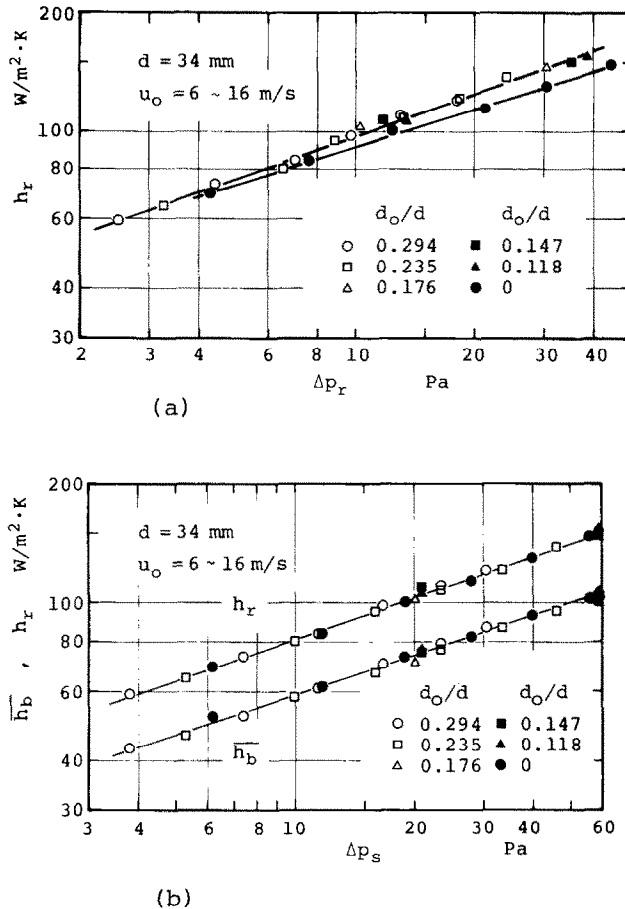


FIG. 8. Correlations of heat transfer coefficient vs R.M.S. fluctuating pressure.

in detail in the previous paper [11], this paper will only give an outline of the characteristics. There is no effect of Reynolds number on the flow characteristics, so the Reynolds number was limited at  $Re = 2.2 \times 10^4$ . Figures 9(a)–(c) show the Strouhal number, the base pressure coefficient and the vortex formation position, respectively. Here the positions of the vortex formation were measured at  $Re = 1.3 \times 10^4$ . As the gap  $g/d$  increases, the value of  $-C_{pb}$  increases and shows a peak at about  $g/d = 0.4$ . This gap is defined as  $G_p$ . The minus base pressure coefficient,  $-C_{pb}$ , has been obtained as a function of  $(g+a)/d$ , and at a critical gap,  $G_c$ , a jump phenomenon takes place. Beyond  $G_c$ , the separated shear layer from the cylinder rolls up in the front region of the splitter plate. The critical gap,  $G_c$ , is a function of the plate length  $a/d$  for  $a/d \leq 0.57$  and a constant for  $a/d \geq 0.74$ . The Strouhal number is nearly equal to that of the single cylinder over the range  $0 \leq g/d < G_p$ , and decreases abruptly near  $g/d = G_p$ . For  $g/d > G_p$ , the Strouhal number decreases considerably as the gap and the length of the plate become larger. Figure 9(c) shows that the inverse of the distance of the vortex formation position varies in the same manner as that of the base pressure coefficient. For  $G_p \leq g/d \leq G_c$ , the separated vortices are formed at the trailing edge of the plate. At  $G_p$  strong vortices are formed and shed at regular

intervals. The vortex formation region is nearest to the cylinder, so the value of  $-C_{pb}$  has a maximum. The interference of the plate on the flow field is different at about  $g/d = G_p$ . In the range of the present experiment, the flow patterns can be classified into three distinct regimes

- pattern A:  $0 \leq g/d < G_p$ ,
- pattern B:  $G_p \leq g/d < G_c$ ,
- pattern C:  $G_c \leq g/d$ .

In the previous paper [11], pattern A was separated into fine regimes, that is, pattern A<sub>1</sub> is for  $a/d < 1.03$  and patterns A<sub>2</sub> and A<sub>3</sub> are for  $a/d \geq 1.03$ . These regimes are treated as an undivided whole in this paper. The effect of the plate on pattern A is small, and the flow field is almost the same as that of the single cylinder. For the single bluff body, a strong correlation is observed between the drag coefficient,  $C_D$ , and the Strouhal number. In general, the Strouhal number increases with a decrease of the drag coefficient (or the base pressure parameter). On the other hand, in the case of the circular cylinder with a splitter plate, both the base pressure parameter,  $K = (1 - C_{pb})^{1/2}$ , and the Strouhal number decrease. The Strouhal number is about half of the value predicted from the above correlation between  $S$  and  $C_D$ . This is the reason, described in the

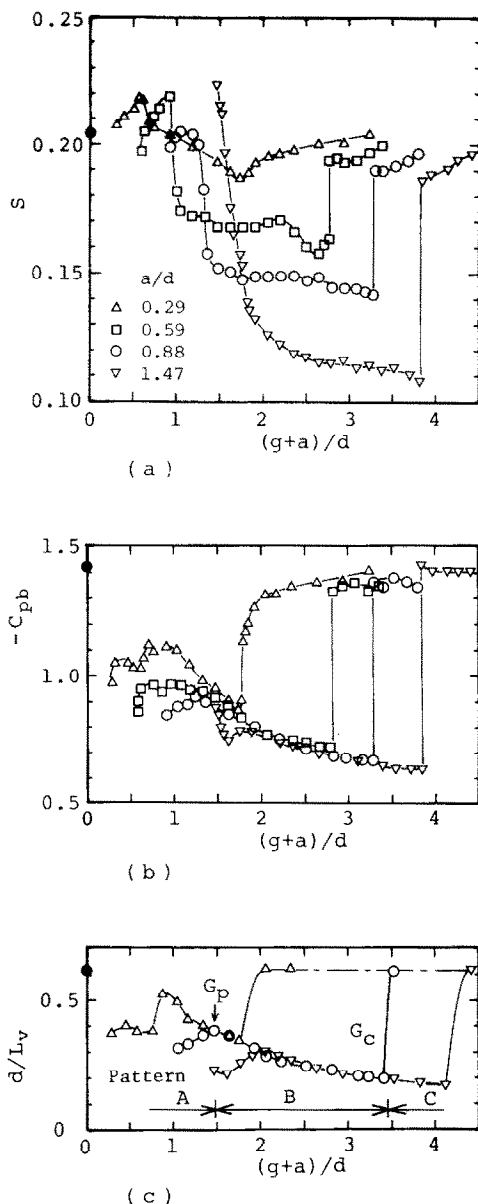


FIG. 9. Flow characteristics: (a) Strouhal number; (b) base pressure coefficient; (c) inverse of vortex formation position.

introduction, that the characteristics of the flow around a circular cylinder with a splitter plate is remarkably different from that of the single cylinder. It is therefore a matter of course that equation (2) obtained for a bluff body can not be applied to a circular cylinder with a splitter plate.

#### 4.2. Heat transfer

The local heat transfer distributions obtained with three different plate lengths for various gaps are shown in Figs. 10(a)–(c). On the front surface of the cylinder, the local heat transfer is scarcely influenced by the plate, while on the rear surface in the separated region, the effect of the plate appears remarkably. As shown in Fig. 10(a), the gap of  $g/d = 0.47, 0.76$ , and  $1.35$  are for

pattern B, the Nusselt numbers on the rear surface decrease as the gaps increase. For the gap of  $g/d = 0.47$  near  $G_p$ , the Nusselt number is larger than that of the single cylinder in the range  $150^\circ \leq \phi \leq 180^\circ$ . For a  $g/d = 1.65$  of pattern C, the profile is nearly equal to that of the single cylinder and independent of the plate. Figure 10(b) represents the case of  $a/d = 0.59$ , the Nusselt number of  $g/d = 0.29$  of pattern A decreases considerably over the separated region. For  $g/d = 0.59$ – $2.09$  of pattern B, those Nusselt numbers are the same as those described for  $a/d = 0.29$ . Figure 10(c) for  $a/d = 0.88$  apart from  $g/d = 0.06$  is the same as that found for Figs. 10(a) and (b) of  $a/d = 0.29$  and  $0.59$ . The heat transfer in the separated region of patterns A, B, and C increase in the order, A, B, C. The Nusselt number of pattern B is proportional to the minus value of the base pressure coefficient,  $-C_{pb}$ . The following points became clear after examining the results. The heat transfer coefficient of pattern A becomes remarkably small and that of pattern B is proportional to the value of  $-C_{pb}$ . Particularly at the gap of  $g/d = G_p$ , the heat transfer coefficient increases considerably and becomes higher than that of the single cylinder in some cases. For pattern C the heat transfer is nearly equal to that of the single cylinder.

Figures 11(a)–(c) show the local heat transfer distributions at a constant base pressure coefficient by the proper combination of  $a/d$  and  $g/d$ . In Fig. 11(a) at  $C_{pb} = -0.96$ , the heat transfer coefficient of pattern A (●) is small, and on pattern B (□, ○), the coefficient for the case of a long plate is higher than that of a short plate. Besides, the heat transfer coefficient increases with a decrease in Strouhal number regardless of patterns A or B. In Fig. 11(b) at  $C_{pb} = -0.875$ , apart from  $a/d = 0.88$  (○), the tendency is the same as that of the case at  $C_{pb} = -0.96$ . In Fig. 11(c) at  $C_{pb} = -0.80$  and  $-0.71$ , the Strouhal number of the long plate is smaller than that of the short plate. In the case of  $C_{pb} = -0.80$ , the heat transfer coefficient of the long plate is larger than that of the short plate, but in the case of  $C_{pb} = -0.71$  the heat transfer coefficients of both plates are nearly equal. From the results described above, one can conclude that the base pressure coefficient,  $C_{pb}$ , that is related to the base pressure parameter,  $K$ , and the velocity along the free stream line at the separation point,  $u_s$ , is one of the important factors governing the heat transfer. In the case of equal values of  $C_{pb}$ , however, the heat transfer coefficients differ remarkably according to the flow patterns. In general, the heat transfer in the same flow pattern increases with a decrease in the Strouhal number. On the other hand, Mabuchi *et al.* [6] reported that selecting  $(g+a)/d = 2.5$  for the chord of the plate from  $a/d = 0.421$  to  $1.465$ , the base pressure coefficient becomes  $C_{pb} = -0.69$ , then the Strouhal number varies from  $S = 0.175$  to  $0.125$  and the heat (mass) transfer coefficient at the rear stagnation point is constant. They derived the conclusion that a change of shedding frequency has no influence on the heat (mass) transfer coefficient at the rear stagnation point. As seen in Fig. 11(a), pattern B

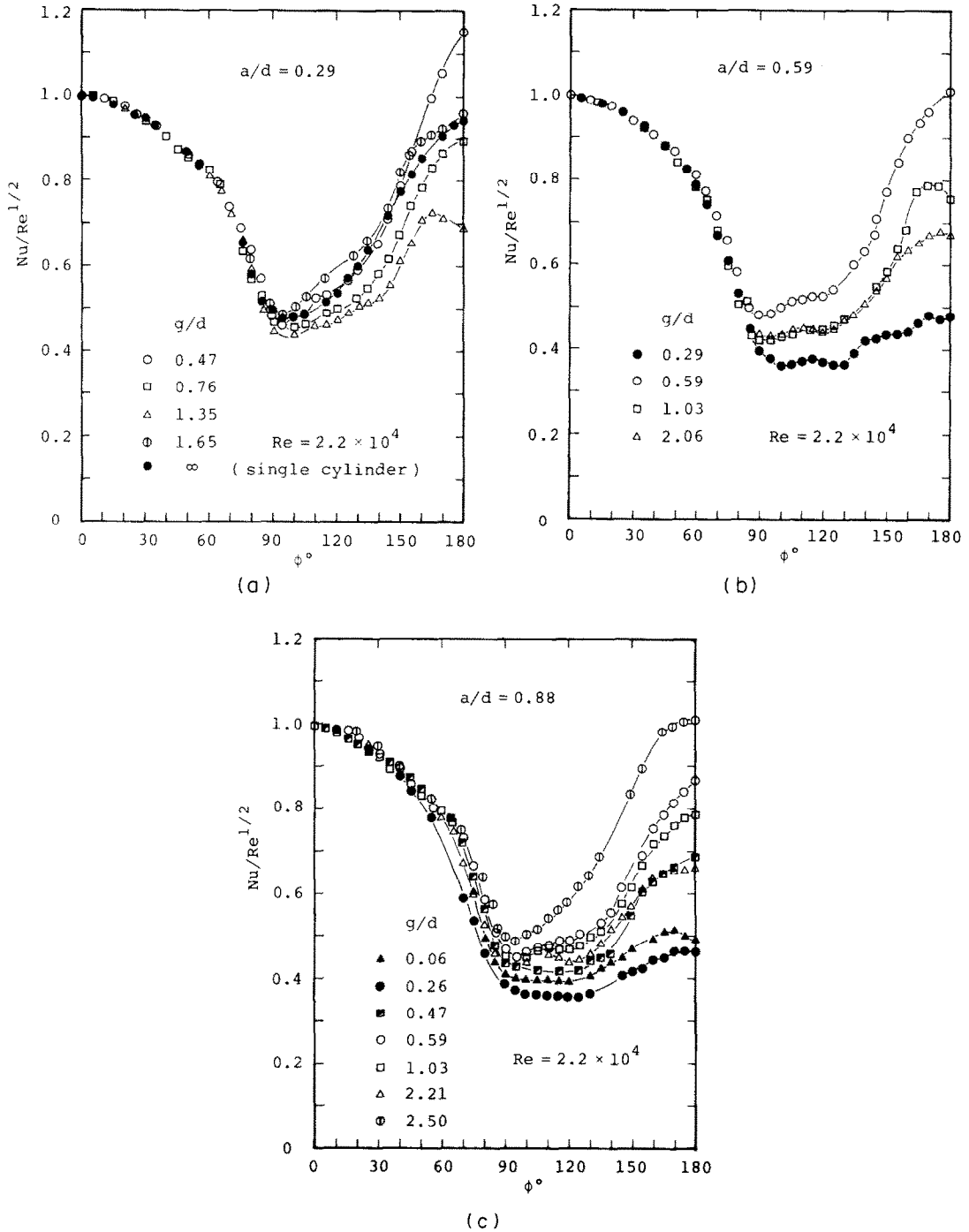


FIG. 10. Variation of local Nusselt number with a splitter plate.

has a tendency to reduce gradually the correlation between the Strouhal number and the heat transfer with a decrease of the value of  $-C_{pb}$ . Viewed from this angle, the result of Mabuchi *et al.* [6] would be understandable, their result, however, was derived from the data under a special condition. This raises questions about the process of deriving their conclusion. Even if their argument should be taken up for the case of  $C_{pb} = -0.96$  in Fig. 11(a), it may give a different conclusion that the heat transfer increases with a decrease in the

Strouhal number. Besides, it is the author's opinion that the Strouhal number should have no influence on the time-averaged heat transfer. With respect to this point, the result of Mabuchi *et al.* [6] is also identical.

It is considered that the Strouhal number is not a directly dominant factor of the heat transfer, but an important factor to characterize the flow field. The change in the Strouhal number would have to be closely related to that in heat transfer. Usually, but not always, the heat transfer coefficient tends to increase with

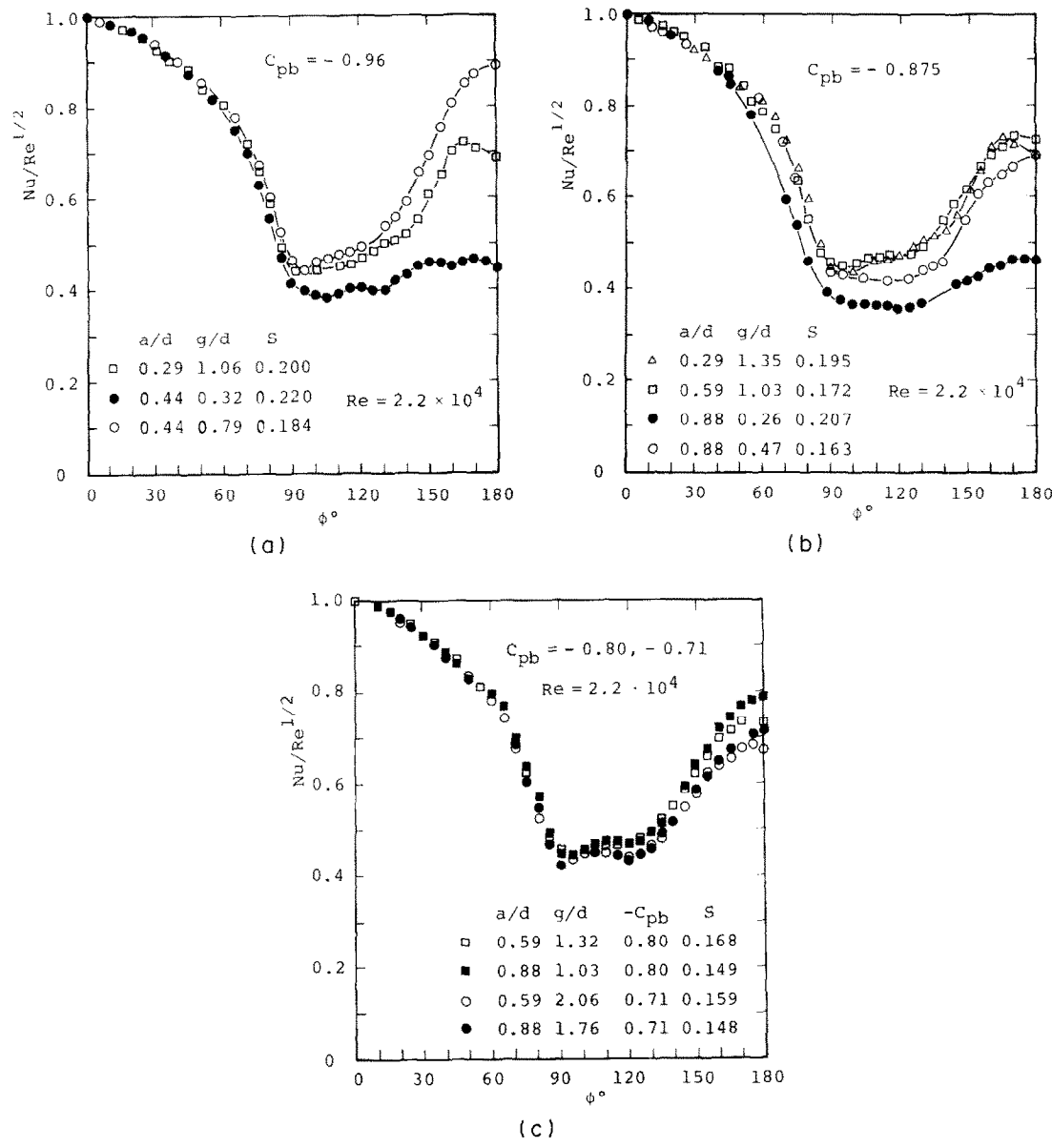


FIG. 11. Distributions of local Nusselt number at constant base pressure.

decreasing the Strouhal number. The larger the value of  $-C_{pb}$ , the more such tendency becomes remarkable.

4.3. Correlation between the R.M.S. fluctuating pressure and heat transfer

In the preceding section, the principle that the local and average heat transfer coefficients on the rear surface are given by the values of the R.M.S. fluctuating pressure at the points of the flow separation and of the rear stagnation, by controlling the shear layer using small cylinders is dealt with. This section is concerned with the examination of this relation for the wake control using the splitter plate. Figure 12 shows the distributions of the R.M.S. fluctuating pressure measured under the same condition as that of the local heat transfer demonstrated in Fig. 11. In the case of

equal base pressure,  $-C_{pb}$ , the smaller the Strouhal number, the larger the R.M.S. value becomes. The R.M.S. value is proportional to the amount of heat transfer. Next the relation between the R.M.S. values,  $\Delta p_s$  and  $\Delta p_r$ , and the free stream velocity,  $u_0$ , is dealt with. In the range  $u_0 = 6\text{--}20\text{ m s}^{-1}$ , they can be represented as

$$\Delta p_s \propto u_0^{2.2}, \quad \Delta p_r \propto u_0^{2.2}. \tag{7}$$

As to the two different wake controls, the nature of the fluid flow in the separated region is the same as the correlation between the R.M.S. fluctuating pressure and the free stream velocity. Moreover, it is of interest in connection with the relation  $Nu \propto Re^{2/3}$  for the heat transfer in the separated region regardless of the wake control. Thus one wishes to examine the quantitative



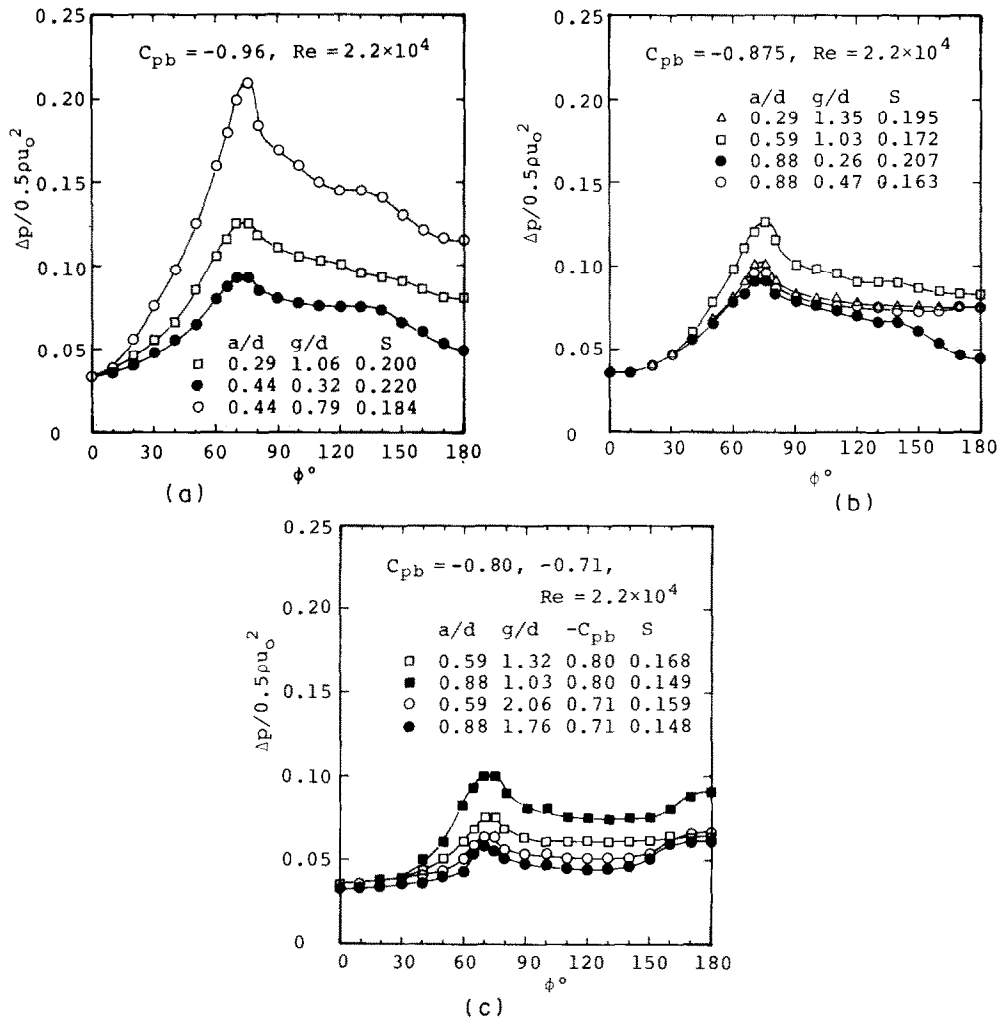


FIG. 12. Distributions of R.M.S. fluctuating pressure at constant base pressure.

relation between the R.M.S. fluctuating pressure at the rear stagnation point and the local and average heat transfer coefficients in the separated regions. The results obtained are shown in Figs. 13(a) and (b). In these figures, the black circles denote the case of the single cylinder, and the solid line is the case of wake control by the small cylinders, as indicated in Fig. 8. The region bounded by dotted lines is patterns A and C, and the other region is pattern B. The data vary widely as compared with Fig. 8. The data of pattern A are near the line of the single cylinder, it is considered that pattern A presents a flow field comparatively similar to that of the single cylinder. For pattern B the vortex formation region is remarkably shifted downstream, then the R.M.S. value decreases considerably. As a result the data points plotted lie above the solid line of the single cylinder. The following conclusions can be drawn from Figs. 13(a) and (b): the correlation of the R.M.S. fluctuating pressure near the separation point with the fluid flow in the vicinity of the rear surface of the cylinder with the splitter plate decreases. These figures were arranged according to the R.M.S. values at the rear stagnation point of the cylinder, and are shown in

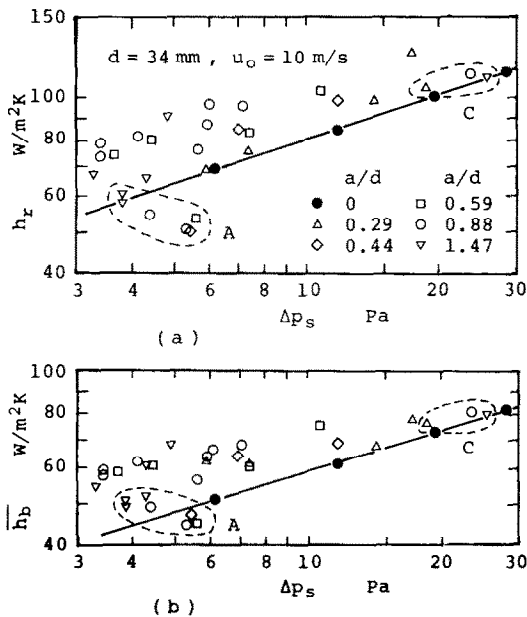


FIG. 13. Correlations of local and average heat transfer coefficients vs  $\Delta p_s$ .

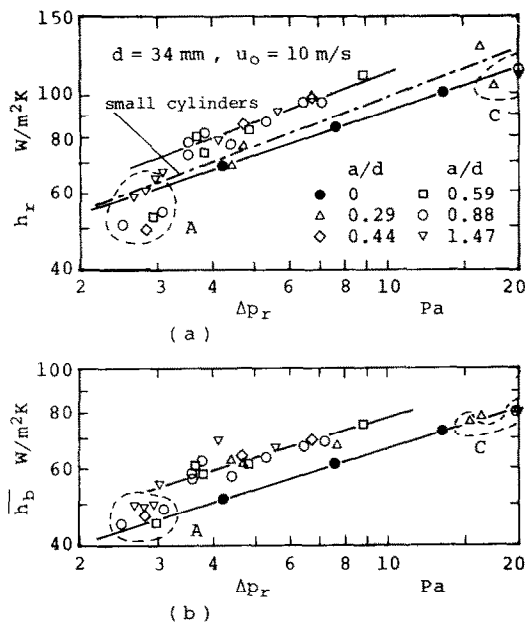


FIG. 14. Correlations of local and average heat transfer coefficients vs  $\Delta p_r$ .

Figs. 14(a) and (b). The plots of data of pattern B give a straight line parallel to that of the single cylinder. They are correlated with the following expressions:

$$h_r \propto \Delta p_r^{0.3}, \quad h_b \propto \Delta p_r^{0.31}. \quad (8)$$

It is worth noting that the data in the case of the single cylinder were obtained by varying the free stream velocity  $u_0$ . On the contrary, the data in the presence of the splitter plate were obtained under the condition of  $u_0 = 10 \text{ m s}^{-1}$ . The changes in R.M.S. values of  $\Delta p_s$  and  $\Delta p_r$  were obtained by varying both the plate length and the gap. An important significance is that equations (5) and (8) hold for the wake control under a constant condition of  $u_0$ . The following equation can be derived from equations (3) and (5) or equations (7) and (8)

$$h \propto \Delta p^{0.31} \propto (u_0^{2.2})^{0.31} = u_0^{0.68}. \quad (9)$$

The above formula is fully consistent with the following equation derived from equation (2)

$$h \propto u_0^{2/3}. \quad (10)$$

## 5. CONCLUSIONS

In connection with the clarification of the heat transfer mechanism in the separated region, the wake of a circular cylinder was controlled in two ways. One way controlled the shake of the shear layers by setting up two small cylinders inside the shear layers. The other controlled the position of the vortex formation region by placing a splitter plate behind the cylinder. The relationship between the heat transfer and the flow characteristics associated with the unsteadiness was

investigated experimentally. The following conclusions were obtained.

(1) The value of the R.M.S. fluctuating pressure,  $\Delta p$ , is one of the most dominant factors of the heat transfer in the separated region.

(2) The factor is given by the value at the separation point,  $\Delta p_s$ , for the case of the small cylinders, and at the rear stagnation point,  $\Delta p_r$ , for the splitter plate. Both the values are related to the local and average heat transfer in the separated region.

(3) The local and average heat transfer coefficients on the rear surface of the cylinder with and without the wake controls are correlated with the values,  $\Delta p_s$  and  $\Delta p_r$ , as follows

$$h_r (\text{or } \bar{h}_b) \propto \Delta p_r^{0.3} \propto \Delta p_s^{0.31}.$$

The relationships hold for the following two cases: one is the change in free stream velocity,  $u_0$ , the other is the change in the value of  $\Delta p$  by the wake controls at a constant velocity.

(4) The factors,  $\Delta p_s$  and  $\Delta p_r$ , are related to the free stream velocity by

$$\Delta p_s, \quad \Delta p_r \propto u_0^{2.2}.$$

## REFERENCES

1. P. D. Richardson, Estimation of the heat transfer from the rear of an immersed body to the region of separated flow, ARL 62-423, Brown University (1962).
2. T. Igarashi and M. Hirata, Heat transfer in separated flows, Part 2: theoretical analysis, *Heat Transfer-Jap. Res.* **6**(3), 60-78 (1977).
3. T. Igarashi and M. Hirata, Heat transfer in separated flows, Part 3: the case of equilateral triangular prisms, *Heat Transfer-Jap. Res.* **6**(4), 13-39 (1977).
4. T. Igarashi and M. Hirata, Heat transfer in separated flows, *Proc. 5th Int. Heat Transfer Conf.*, Vol. 2, pp. 300-304 (1974).
5. R. A. Seban and A. M. Levy, The effect of a downstream splitter plate on the heat transfer from a circular cylinder normal to an air stream, WADC TR 57-479 (ASTIA AD 155765) (1957).
6. I. Mabuchi, M. Hiwada and M. Kumada, Some experiments associated with heat transfer mechanism in turbulent separated region of a cylinder, *Proc. 5th Int. Heat Transfer Conf.*, Vol. 2, pp. 315-319 (1974).
7. M. Hiwada, K. Niwa, M. Kumada and I. Mabuchi, Effects of tunnel blockage on local mass transfer from a circular cylinder in cross flow, *Heat Transfer-Jap. Res.* **8**(3), 37-51 (1979).
8. T. Igarashi, Unsteadiness in separated flow region, *Proc. 16th National Heat Transfer Symp. of Japan*, pp. 40-42 (1979) (in Japanese).
9. T. Igarashi, Unsteadiness of the flow and heat transfer in separated region of a circular cylinder, *Proc. 17th National Heat Transfer Symp. of Japan*, pp. 10-12 (1980) (in Japanese).
10. T. Igarashi, Fluid flow and heat transfer in the separated region of a circular cylinder with wake control, *Heat Transfer-Jap. Res.* **11**(3), 1-16 (1982).
11. T. Igarashi, Investigation on the flow behind a circular cylinder with a wake splitter plate, *Bull. J.S.M.E.* **25**(202), 528-535 (1982).

RELATION ENTRE LE TRANSFERT THERMIQUE ET LA  
FLUCTUATION DE PRESSION DANS LA REGION DE SEPARATION  
D'UN CYLINDRE CIRCULAIRE

**Résumé**— Le sillage d'un cylindre circulaire est contrôlé de deux façons : en plaçant deux petits cylindres dans les couches séparées et en plaçant une plaque derrière le cylindre. L'une contrôle l'agitation des couches de cisaillement, l'autre la région de formation du tourbillon. On étudie la relation entre le transfert thermique dans les régions de séparation et les caractéristiques de l'écoulement, en rapport avec les composantes fluctuantes de l'écoulement. On trouve que la R.M.S. de la pression fluctuante au point d'arrêt arrière est un des facteurs prédominants du transfert thermique dans les régions séparées.

BEZIEHUNG ZWISCHEN WÄRMEÜBERGANG UND DRUCKSCHWANKUNGEN  
IM ABLÖSEGEBIET EINES KREISZYLINDERS

**Zusammenfassung**— Der Nachlauf eines Kreiszylinders wurde auf zwei Arten beeinflusst : durch Anbringen zweier kleinerer Zylinder innerhalb der abgelösten Scherungsschichten und durch Anbringen einer Trennplatte hinter dem Zylinder. Im ersten Fall wird die Ablösungsfläche der Scherungsschichten beeinflusst, im zweiten das Wirbelbildungsgebiet. Die Beziehung zwischen dem Wärmeübergang im Ablösegebiet und dem Strömungsverhalten in bezug auf die Schwankungskomponenten der Strömung wurde untersucht. Es zeigte sich, daß der quadratische Mittelwert der Druckschwankungen im hinteren Staupunkt einer der stärksten Einflußfaktoren auf den Wärmeübergang im Ablösegebiet war.

КОРРЕЛЯЦИЯ МЕЖДУ ТЕПЛОВЫМ ПОТОКОМ И ПУЛЬСАЦИЯМИ ДАВЛЕНИЯ В  
ОТРЫВНОЙ ОБЛАСТИ ТЕЧЕНИЯ ЗА КРУГОВЫМ ЦИЛИНДРОМ

**Аннотация**— След за круговым цилиндром исследовался двумя способами: помещением двух небольших цилиндров в область отрыва пограничных слоев и установкой за цилиндром пластины для разделения потока. В первом случае осуществляется контроль за пульсацией пограничных слоев, во втором – за областью образования вихрей. Исследуется соотношение между величиной теплового потока в отрывной области и характеристиками течения с учетом их пульсирующего характера. Найдено, что среднеквадратичная величина пульсаций давления в задней критической точке является одним из определяющих параметров в процессе переноса тепла в отрывной области потока.